DOI: https://doi.org/10.1016/j.biortech.2018.09.062

# Solvent and catalyst effect in the formic acid aided Lignin-to-liquids

Mikel Oregui-Bengoechea*[a,b], Inaki Gandarias[b], Pedro L. Arias[b] and Tanja Barth[a]

[a] *Department of Chemistry, University of Bergen, Allégaten 41, 5007 Bergen, Norway*

[b] *Department of Chemical and Environmental Engineering, School of Engineering, University of the Basque Country (EHU/UPV), C/Alameda Urquijo s/n,48013 Bilbao, Spain*

**Abstract**

The effect of the type of solvent, ethanol or water, and a Ru/C catalyst were studied in the formic acid aided lignin conversion. The best results were obtained in the presence of the Ru/C catalyst and using ethanol as solvent at 300 °C and 10 h (i.e. 75.8 wt.% of oil and 23.9 wt.% of solids). In comparison to the water system, the ethanol system yields a significantly larger amount of oil and, at 300 °C and 10 h, a smaller amount of solids. The main reasons for this positive effect of the ethanol solvent are i) the formation of ethanol-derived esters, ii) C-alkylations of lignin fragments and iii) the generation of more stable lignin derivatives. The Ru/C exhibits significantly higher lignin conversion activity compared to other Ni-based catalysts, especially at 300 °C, which is related to the enhanced activity of the $Ru^0$ sites towards hydrogenolysis, hydrodeoxygenation and alkylation reactions.

**Keywords:** lignin, LtL, formic acid, Ru/C, bio-oil, ethanol, water

## 1. Introduction

The transition from a fossil-based to a more sustainable economy is the major challenge that faces today´s society. While energy can be produced from different renewable sources, other crude oil based consumer products (i.e. chemicals) can only be produced from biomass (Popa, 2018). In particular, the lignocellulosic biomass found in both agricultural and forestry residues is an abundant and versatile resource with enormous potential for replacing conventional fossil sources (IEA, 2012). However, processing large quantities of sugars into fuels and chemicals – from the cellulose and hemicellulose- will generate a huge amount of lignin waste (Zakzeski et al., 2010). Besides, as lignin is the only renewable source of aromatic hydrocarbons, its efficient conversion is crucial for the production of renewable aromatic-derived consumer products (Lange et al., 2013; Zakzeski et al., 2010). Hence, the viability of future biorefineries is highly dependent on the development of inexpensive lignin conversion strategies.

Among all lignin conversion methods, catalytic hydroprocessing is one of the most popular and efficient strategies applied in lignin deconstruction (Li et al., 2015). Highly promising building block chemicals such as low depolymerized lignin, catechol, guaiacol and phenol could be obtained (Abioye and Ani, 2015; Azadfar et al., 2015; Kleinert and Barth, 2008). Further upgrading of such compounds can lead to hydrocarbon value-added commodity chemicals and fuels (Li et al., 2015).

The Lignin-to-Liquids (LtL) process is a relatively new lignin hydroprocessing method that can effectively convert the biopolymer in a highly deoxygenated bio-oil (Kleinert et al., 2009; Kleinert and Barth, 2008). This method involves the use of formic acid (FA) together with a solvent, either ethanol or water, and meets all the sustainability and

45 green process criteria, since all the reactants can be obtained from renewable resources.
46 Formic acid is one of the main sub-products from the cellulose and hemicellulose
47 hydrolysis and sugar conversion processes (Hayes et al., 2008; J??nsson et al., 2013).
48 Ethanol can be produced through the conversion of the cellulose and hemicellulose
49 fractions of lignocellulose (Chandrakant and Bisaria, 1998). Water, in particular, is a
50 promising solvent choice due to its low cost and large availability. However, to make
51 this process competitive with fuels and chemicals obtained from crude oil, some
52 important process parameters (i.e. reaction time and temperature) need to be improved.

53 One possibility to address these challenges is the use of heterogeneous catalysis.
54 Traditionally mixed sulfides of NiMo, NiW, CoMo and CoW are widely used in
55 hydrotreating processes (Li et al., 2015). However, such catalysts could deactivate due
56 to the high oxygen content of lignin (Wang et al., 2011) and induce the sulfur
57 contamination of the bio-oil products (Nie et al., 2014). Furthermore, these catalyst are
58 known to undergo severe deactivation in the presence of water (E. Laurent and Delmon,
59 1994; Etienne Laurent and Delmon, 1994). Thus, noble metal-based catalyst would be
60 a preferred choice for the conversion of lignin in both water and ethanol. The activity of
61 a wide variety of noble metal-based catalysts have been studied for the LtL or for
62 similar lignin conversion processes, such as $Rh/Al_2O_3$ (Oregui Bengoechea et al., 2017),
63 $Pd/Al_2O_3$ (Oregui Bengoechea et al., 2017), $Ru/Al_2O_3$ (Oregui Bengoechea et al., 2017),
64 Rh/C (Pepper and Lee, 1969), Pd/C (Pepper and Lee, 1969), Ru/C (Huang et al., 2018;
65 Kloekhorst et al., 2015) and Pt/C (Xu et al., 2012).

66 We recently reported a study comparing the activity of $Ru/Al_2O_3$, $Rh/Al_2O_3$ and
67 $Pd/Al_2O_3$ catalyst in the LtL reaction (Oregui Bengoechea et al., 2017). Higher oil
68 yields were obtained when using Ru as the active metal (Oregui Bengoechea et al.,
69 2017). Regarding the support, hydrotreating catalyst supported on activated carbons

(ACs) are promising alternatives to traditional metal oxide supports. This is due to: (i) less coking (Boorman et al., 1992; Vissers et al., 1987); (ii) lower cost; (iii) the possibility of recovering the active metals from spent catalysts by burning off the carbon, and (iv) the possibility of being produced from lignocellulosic biomass, lignin, or even solid organic residues of the LtL process (Abioye and Ani, 2015; Hao et al., 2017, 2014; Suhas et al., 2007).

In this study, we analyze the effect of the type of solvent, either ethanol or water, for the non-catalyzed and the Ru/AC catalyzed LtL process. Several studies have focused in the catalytic LtL process in either ethanol (Huang et al., 2018; Kloekhorst and Heeres, 2015; Oregui-Bengoechea et al., 2017; Oregui-Bengoechea et al., 2017b; Xu et al., 2012) or water (Liguori and Barth, 2011; M. Oregui Bengoechea et al., 2017; Oregui Bengoechea et al., 2015). The effect of the solvent type for the non-catalyzed LtL process has also been briefly analyzed (Løhre et al., 2016). However, to the best of our knowledge, no systematical analysis of the distinctive solvent effect of ethanol and water has been carried out for the catalyzed LtL process.

## 2. Materials and methods

### *2.1 Chemicals*

Formic acid (>98%), tetrahydrofuran (THF) (>99.9%), ethyl acetate (EtAc) (99.8%), hexadecane (>99.8 %) and anhydrous sodium sulphate (>99.0 %) were purchased from Sigma Aldrich and used as supplied. Anhydrous $RuCl_3$ and activated carbon (AC) were purchased from Strem Chemicals Inc.

Rice straw lignin from strong acid carbohydrate dissolution pre-treatment was received from the Technical College of Bergen. The lignin was ground, and sieved (<500 μm) prior to use. The inorganic components of the lignin were also determined.

94 *2.2 Catalyst*

95 *2.2.1 Synthesis of the catalysts*

96 The Ru/AC catalyst was prepared by incipient-wetness impregnation of the AC support
97 with an aqueous solution of $RuCl_3$. Prior to impregnation, the AC was dried under
98 vacuum at 160 °C for 12 h. After drying, 4 g. of the AC support were impregnated with
99 20 mL of an aqueous solution of $RuCl_3$ (0.0335 M). The nominal Ru loading was thus
100 4.3 wt.%, so that the number of moles of Ru resembles de number of Ni moles of a Ni-
101 based catalysts used in a previous study (Oregui-Bengoechea et al., 2017b). After
102 impregnation, the catalyst was dried at 105 °C for 20 min. The solid was then thermal-
103 treated under a $N_2$ flow (10 mL/min) at 470 °C for 2 h using a heating ramp of 2
104 °C/min. Finally, the catalyst was activated in a $H_2/N_2$ (10/90, vol/vol) flow (10 mL/min)
105 at 450 °C for 2 h with the same heating ramp of 2 °C/min.

106 The catalyst was characterized by $N_2$-adsorption, X-ray diffraction (XRD), CO-
107 chemisorption, TPR of the non-activated Ru/AC catalyst and ICP-EOS.

108 *2.3 LtL experiments*

109 *2.3.1 Experimental set-up*

110 Rice straw lignin (2 g), formic acid (1.5 g), the catalyst (0.2 g), if any, and either ethanol
111 (2.5 g) or water (2.5 g), were added to a stainless steel reactor (Parr 4742 non-stirred
112 reactor, 25 mL volume). The reactor was closed and heated in a CarboliteTM LHT oven
113 at 300 °C for 10 h (LT conditions), or at 340 °C for 6 h (HT conditions). The reactor
114 was not purged after closing. Two replicates were carried out for each experiment, and
115 the results refer to the related average. In case that the oil or solid yield values differed
116 more than 3.0 percentage points (wt.% points), an additional experiment was carried

117 out. The experiments are named after the type of catalyst, the type of solvent, either
118 ethanol or water and the reaction conditions.

119 *2.3.2 Work-up procedure*

120 After the reaction, the reactor was removed from the oven and cooled to ambient
121 temperature by natural convection. The reactor was opened and the liquid reaction
122 mixture was extracted with a solution of ethyl acetate-tetrahydrofurane (90:10). The
123 solid phase (unreacted lignin, inorganic and organic lignin residues and catalyst) was
124 filtered off and dried at ambient conditions for 2 days before weighing.

125 The subsequent work-up steps differed depending on the solvent of choice. For the
126 water system, two well-separated liquid phases were obtained (organic top phase and
127 aqueous bottom phase). The phases were separated by decantation and the organic
128 phase was dried over $Na_2SO_4$ and concentrated at reduced pressure (ca. 160 mbar) at 40
129 °C. For the ethanol system, a single dark-brown organic liquid phase was obtained. This
130 was dried over anhydrous $Na_2SO_4$ and concentrated at a reduced pressure (ca. 160
131 mbar) at 40 ° C.

132 The final oil and solid yields were determined by weight (amount of oil or solids
133 (g)/amount of introduced lignin (g)) after the work-up procedure was completed. The
134 solid yield for the catalyzed systems was calculated after subtracting the amount of
135 catalyst introduced, hence, the solid yield referred to the sum of the organic solids
136 (hydrochar) and the inorganic lignin ashes. The oil was characterized by elemental
137 analysis, GC-MS and GPC-SEC. GPC-SEC results are reported as average $M_w$ only, due
138 to very similar shapes of the chromatogram peaks for all samples.

139

## 3. Results and Discussion

### *3.1 Catalyst characterization*

The $N_2$ adsorption-desorption isotherm of the AC bare support and its pore size distribution indicate that the AC is mainly of microporous nature with some small size mesopores (i.e. 2-4 nm). The specific surface area of the AC bare support is of 1415 $m^2/g$. After supporting the Ru species, the surface area decreases to 1185 $m^2/g$, however, the nature of the solid (i.e. microporous solid with some small size mesopores) is not altered, as observed from the $N_2$ adsorption-desorption isotherm.

The XRD diffractograms of the AC support and the activated Ru/AC exhibit a sharp crystalline peak at $2\theta = 26.2^{\circ}$ (PDF: 00-026-1076) corresponding to graphite and a broad scattering peak at $2\theta = 20^{\circ}$- $30^{\circ}$ corresponding to amorphous carbons (Divakar et al., 2007; Liu et al., 2012). These diffraction peaks correspond to the AC activated carbon. Besides, the Ru/AC catalyst exhibits additional diffraction peaks corresponding to the hexagonal $Ru^0$ structure. The diffraction peaks at $2\theta = 38.4^{o}$, $42.2^{o}$ and $43.9^{o}$ correspond to the (1 0 0), (0 0 2) and (1 0 1) planes of the hexagonal $Ru^0$ structure (PDF: 00-006-0663). An additional diffraction peak around $2\theta = 67.7^{o}$ typical for hexagonal Ru structure is also observed (PDF: 00-006-0663). To further confirm the oxidation state of the Ru species during the LtL process a TPR of the non-activated Ru/AC catalyst was carried out. The Ru/AC catalysts exhibits two main reduction peaks: a low temperature peak centered around 100 ˚C and a high temperature broad peak centered around 375 ˚C. The low temperature peak is attributed to the reduction of Ru oxide species to $Ru^0$, while the high temperature peak is associated with the degradation of the AC carbon; consumption of $H_2$ associated with $CH_4$ formation (Rossetti et al., 2003). The Ru catalyzes the breaking of the weakest C-C bonds at the surface of active carbon giving rise to this high temperature peak (Rossetti et al., 2003).

Thus, the TPR analysis suggests that under LtL conditions, high temperatures in a highly reducing environment due to formic acid decomposition, the Ru species of the activated Ru/AC catalyst will be mainly in the form of $Ru^0$. The Ru/AC catalyst has a Ru loading of 3.7 wt.%, as measured by ICP-EAS. The amount of chemisorbed CO is 4.4 µmol CO/g catalyst, as measured by CO-chemisorption. Thus, considering a CO:Ru stoichiometry of 0.6:1(Kowalczyk et al., 2008), the number of $Ru^0$ active sites is 7.3 µmol/g catalyst.

## *3.2 LtL results*

### *3.2.1 Oil, solid and lignin recovery yield*

The LtL-process results for the non-catalyzed (NC), AC and Ru/AC catalyzed experiments are summarized in Table 1. These results correspond to the average of both replicates. No significant differences are observed within the replicates, which confirms that the catalytic LtL experiments are highly reproducible. Note that the content of inorganic ashes of the lignin (i.e. rice straw lignin) used in these experiments is 14.9 wt.%; therefore, the actual organic solid yield is considerably smaller than the solid yield shown in the table. The recovery yield presented in Table 1 refers to the proportion of lignin that has been recovered in the form of oil and solid. It is an indirect measurement of the amount of lignin converted into gas and/or the oil and solid that may have been lost during the work-up procedure.

185 Table 1: Oil, solid and lignin recovery yields, and elemental analysis and $M_w$ of the oils
186 for the NC, AC and Ru experiments.

| Entry | Experiment A[a]-B[b]-X[c] | Oil Yield (wt.%)[d,e] | Solid Yield (wt.%)[d,e] | Lignin recovery yield (wt %)[d,e] | $M_w$[e] (Da) | Elemental analysis of the oils | |
|---|---|---|---|---|---|---|---|
| | | | | | | H/C[e] | O/C[e] |
| 1 | NC-E-HT | 36.0 | 43.6 | 79.6 | 347 | 1.24 | 0.13 |
| 2 | NC-W-HT | 30.5 | 32.8 | 63.3 | 222 | 1.13 | 0.16 |
| 3 | NC-E-LT | 49.3 | 28.3 | 77.5 | 552 | 1.18 | 0.17 |
| 4 | NC-W-LT | 33.6 | 44.3 | 77.8 | 280 | 1.13 | 0.20 |
| 5 | AC-E-HT | 44.4 | 35.7 | 80.1 | 340 | 1.35 | 0.15 |
| 6 | AC-W-HT | 31.1 | 42.3 | 73.3 | 225 | 1.21 | 0.15 |
| 7 | AC-E-LT | 50.7 | 30.6 | 81.9 | 483 | 1.22 | 0.18 |
| 8 | AC-W-LT | 31.0 | 54.8 | 85.8 | 280 | 1.26 | 0.20 |
| 9 | Ru-E-HT | 72.0 | 22.9 | 94.9 | 415 | 1.33 | 0.14 |
| 10 | Ru-W-HT | 56.0 | 23.1 | 79.1 | 319 | 1.32 | 0.17 |
| 11 | Ru-E-LT | 75.8 | 23.9 | 99.6 | 498 | 1.33 | 0.20 |
| 12 | Ru-W-LT | 42.9 | 39.9 | 82.8 | 360 | 1.23 | 0.17 |

187 [a] Type of catalyst: non-catalyzed (NC), bare activated carbon (AC) and activated Ru/AC
188 catalyst (Ru) [b] Type of solvent: ethanol (E) or water (W) [c] Reaction conditions: 340 °C
189 and 6 h (HT) and 300 °C and 10 h (LT) [d] Relative to lignin input [e] Average value of the
190 replicates

191 The results obtained for the non-catalyzed (NC) experiments are shown in Table 1
192 (*entries 1-4*). The lignin recovery yields are 77 wt.% or above, except for the NC-W-HT
193 experiment, where only 63.3 wt.% of the initial lignin was recovered in the form of oil
194 and solid. At both reaction conditions, HT and LT, the oil yields for the ethanol system
195 are higher than the ones obtained for the water system (Figure 1a). For the HT
196 experiments (e.g. 340 ˚C and 6 h), the oil yield for the ethanol system is 36.0 wt.%,
197 (NC-E-HT experiment), while only 30.5 wt.% for the water system (NC-W-HT
198 experiment). This difference is even higher at LT conditions (e.g. 300 ˚C and 6 h), with

an oil yield 49.3 wt.% for the NC-E-LT experiment and only 33.6 wt.% for the NC-W-LT.

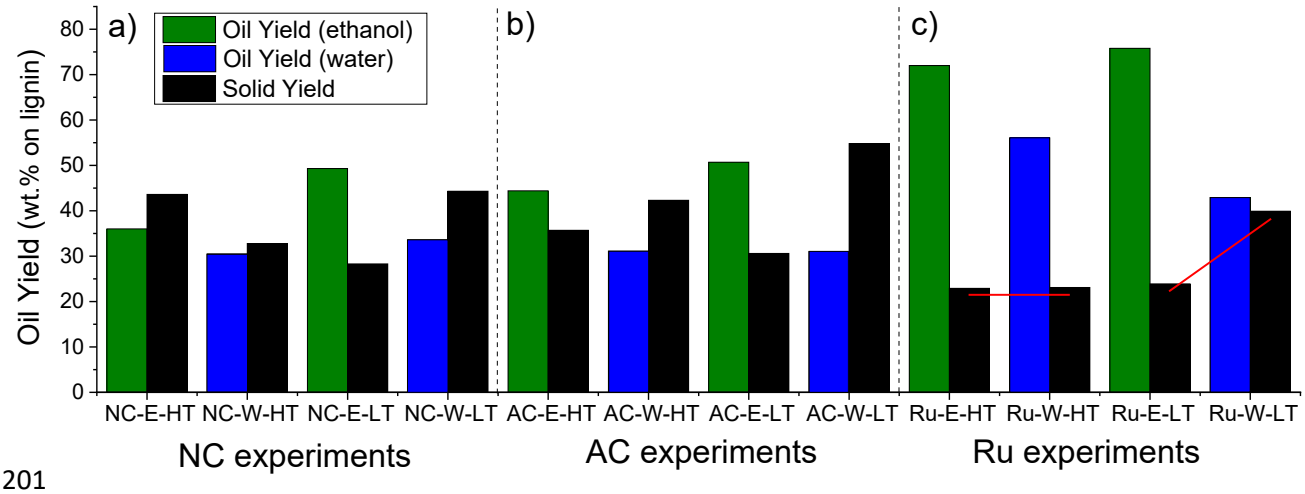


Figure 1. Oil and solid yield for the (a) NC, (b) AC and (c) Ru experiments. Oil yield using ethanol as solvent (green), oil yield using water as solvent (blue) and solid yield (black).

The results obtained for the AC experiments are shown in Table 1 (*entries 5-8*). All lignin recovery yields, except for the AC-W-HT experiment, are above 80 wt.%. The oil and solid yields are comparable to the ones obtained for the NC experiments, except for the AC-E-HT experiment, where a higher oil and lower solid yields are obtained in comparison to the NC counterpart. These results indicate that the AC support exhibits some activity towards lignin conversion, but only for the ethanol system and at HT conditions. In any case, as already observed for the NC experiments, the oil yields obtained for the AC ethanol system are again considerably higher than the ones obtained for the AC water system (Figure 1b). This difference is 13.3 percentage points for the HT experiments, and 19.7 percentage points for the LT. The solid yields are comparable to the ones obtained for the NC experiments, except for the AC-E-HT experiment.

The results obtained for the Ru/AC catalyst are shown in Table 1 (*entries 9-12*). The lignin recovery yields are close to 100 wt.% in the case of the ethanol experiments, and around 80 wt.% in the case of water. The Ru/AC catalyst has a substantial positive effect on the LtL process for all cases: for both reaction systems (i.e. water and ethanol) and at both reaction conditions (i.e. HT and LT). Considerably higher oil yields and considerably lower solids yields are obtained for the Ru experiments in comparison to their AC and NC counterparts (Table 1, *entries 1-12*). This indicates that the Ru/AC catalyst has a positive effect on the de-polymerization of the lignin biopolymer and the stabilization of the lignin fragments.

As observed, the effect of the type of solvent in the Ru/AC catalyzed results is still significant (Figure 1c). Considerably higher oil yields are again obtained when ethanol is used as a solvent. The Ru/AC catalyzed experiments are also affected by the reaction conditions (i.e. HT or LT), especially the solid yield. At HT conditions, the oil yields are 75.2 wt.% for the ethanol system (Ru-E-HT) and only 56.0 wt.% for the water system (Ru-W-HT). Remarkably, both experiments yield comparable amount of solids, with 20.3 wt.% for the Ru-E-HT and 23.1 wt.% for the Ru-W-HT (Figure 1c). At LT conditions, the ethanol system yields considerably larger amount of oil, 75.8 wt.% for the Ru-E-LT while only 42.9 wt.% for the Ru-W-LT. However, at LT conditions, the ethanol system yields significantly smaller amount of solids: 23.9 wt.% of solids for the Ru-E-LT while 39.9 wt.% for the Ru-W-LT (Figure 1c).

### *3.2.2 Oil properties ($M_w$ and H/C and O/C ratios) and its composition (GC-MS)*

The type of solvent system also affects the quality of the bio-oil and its composition. When using ethanol as solvent, oils with significantly higher average molecular weight ($M_w$) are obtained. At HT conditions the $M_w$ of the oil is of 347 Da for the NC-E-HT experiment, while only 222 Da for the NC-W-HT. At LT, this difference is more pronounced: 552 Da for the NC-E-LT while only 280 Da for the NC-W-LT (Figure 2, *above*). The H/C and O/C ratios of the NC oils presented in Table 1 (*entries 1-4*) indicate that the ethanol system yields more hydrodeoxygenated oils than the water system. At both HT and LT conditions, the ethanol oils exhibit higher H/C and in most cases lower O/C ratios (Figure 2, *below*).

248

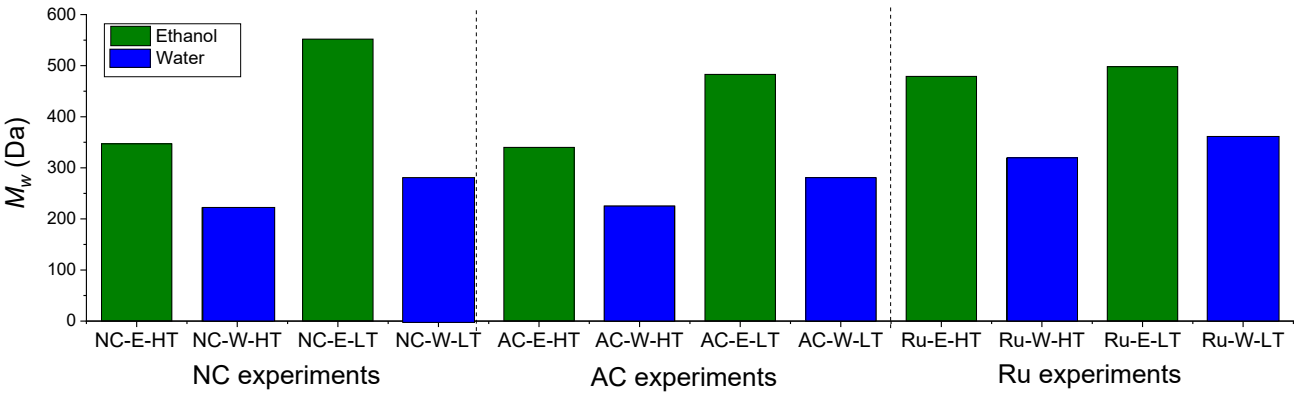


249

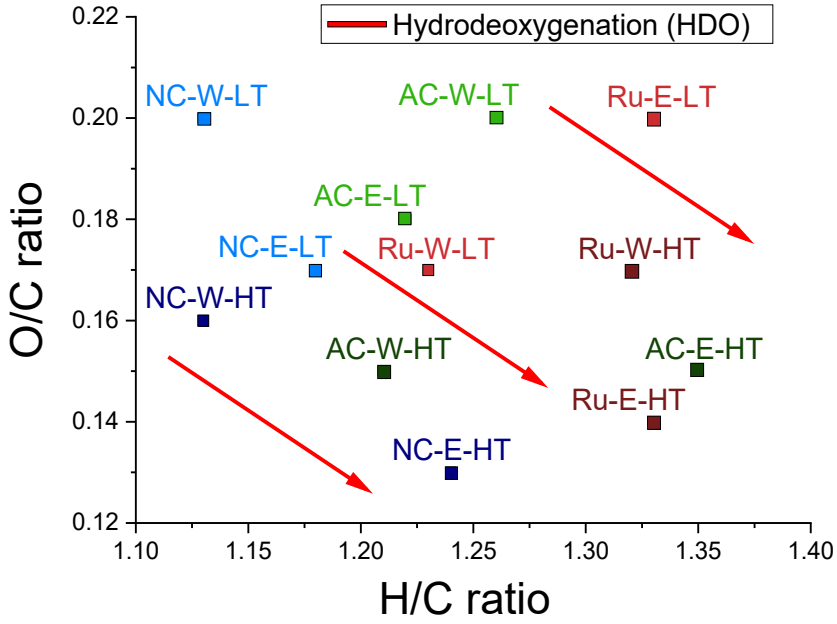


250 Figure 2. Average molecular weight of the NC, AC and Ru experiments (*above*) and

251 H/C and O/C ratio of the NC, AC and Ru experiments (below).

252

253 **Table 2:** Semi-quantitative GC-MS analysis of the HT oils

| Compound | Experiment (Oil) | | | | | |
|---|---|---|---|---|---|---|
| | NC-E-HT | NC-W-HT | AC-E-HT | AC-W-HT | Ru-E-HT | Ru-W-HT |
| 2-ethyl-1-hexanol | 2.82 | 0.31 | 2.11 | 1.08 | 0.88 | 0.75 |
| Ethyl benzoate | 2.64 | –[a] | 2.28 | –[a] | 1.05 | –[a] |
| Diethyl succinate | 0.69 | –[a] | 0.82 | –[a] | 0.37 | –[a] |
| Phenol | 0.56 | 0.70 | 0.72 | 0.96 | 0.28 | 1.34 |
| o-Cresol | 0.36 | 0.33 | 0.41 | 0.46 | 0.15 | 0.36 |
| p-Cresol | 0.44 | 0.85 | 0.49 | 1.19 | 0.23 | 1.25 |
| o-Ethylphenol | 0.51 | –[a] | 0.60 | –[a] | 0.31 | –[a] |
| p-Ethylphenol | 0.62 | 0.91 | 0.70 | 1.21 | 0.35 | 1.35 |
| p-Propylphenol | –[a] | –[a] | –[a] | –[a] | 0.16 | 1.07 |
| EtMtP[b] | 0.85 | 0.29 | 1.15 | 0.45 | 0.41 | –[a] |
| Diethylphenol | 0.71 | –[a] | 1.18 | –[a] | 0.86 | –[a] |
| Propofol | –[a] | –[a] | –[a] | –[a] | 0.25 | –[a] |
| Catechol | –[a] | 0.31 | –[a] | 0.57 | –[a] | –[a] |
| Methylcatechol | –[a] | 0.49 | –[a] | 0.59 | –[a] | –[a] |
| Ethylcatechol | –[a] | 0.50 | –[a] | 0.52 | –[a] | –[a] |
| dMthdMtB[c] | –[a] | –[a] | –[a] | –[a] | 0.51 | –[a] |
| dMtEtdMthB[d] | –[a] | –[a] | –[a] | –[a] | 0.41 | –[a] |
| tEtB[e] | –[a] | –[a] | –[a] | –[a] | 0.22 | –[a] |
| pMtB[f] | –[a] | –[a] | –[a] | –[a] | –[a] | 0.54 |
| 5-hydroxyindane | –[a] | 0.61 | –[a] | 0.62 | –[a] | 0.86 |
| EtProp[g] | –[a] | –[a] | –[a] | –[a] | –[a] | 0.77 |
| MtNaph[h] | –[a] | 0.27 | –[a] | 0.43 | –[a] | –[a] |

254 [a]Low intensity peak or undetected compound [b]EtMtP: 2-ethyl-5-methylphenol

255 [c]dMthdMtB: 1,4-Dimethoxy-2,3-dimethylbenzene [d]dMtEtdMthB: 2-(1,1-

256 dimethylethyl)-1,4-dimethoxybenzene [e]tEtB: 1,2,4,5-tetraethylbenzene [f]pMtB:

257 1,2,3,5,6-pentamethylbenzene [g]EtProp: 2′-Ethylpropiiophenone [h]MtNaph: 2-methyl-1-

258 naphthalenol

259 The semi-quantitative analysis of the oils based on the relative abundance of each

260 compound ($A_I/A_S$) is presented in Table 2 and Table 3. The relative abundance of a

261 compound ($A_I/A_S$) is defined as the ratio between the area of the peak for a certain

262 compound ($A_I$) and the area of the internal standard peak ($A_S$). Note that in the GC-MS

263 analysis only the most volatile oil components, those compounds with lower molecular
264 weight, can be identified. Thus, for those oils with low $M_w$ values, the composition
265 obtained by GC-MS analysis will be more representative of the overall composition.
266 The NC-E-HT, NC-W-HT, NC-E-LT and NC-W-LT oils exhibit GC peaks that can be
267 assigned to compounds coming from the capillary column.

268 At HT, there are significant differences between the ethanol and water system in the
269 composition of the oil, as observed from the semi-quantitative GC-MS analysis (Table
270 2). The compounds with the highest relative abundance in the NC-E-HT oil are 2-ethyl-
271 1-hexanol and ethyl benzoate. Diethyl succinate and ethyl-and methyl-substituted
272 phenols are also found in high relative abundance. In the case of the water system, NC-
273 W-HT experiment, the compounds with the highest relative abundance are p-
274 ethylphenol and p-cresol. Methyl and ethyl substituted phenols and highly polar
275 oxygenated compounds such as catechols are also detected. Compounds such as 5-
276 hydroxyindane and 2-methyl-1-naphthalenol have also been identified. In the case of the
277 NC-W-HT experiment ethyl substituted compounds such as ethylphenol (i.e. sum of
278 ortho- and para-substituted), 2-ethyl-5-methylphenol and diethylphenol are less
279 abundant than in the NC-E-HT.

280 Unlike HT oils, the oils produced at LT conditions, Table 3, contain high concentrations
281 of ethoxy- and methoxyphenols (i.e. guaiacols). Still, significant compositional
282 differences are observed between the ethanol and the water system. For the ethanol
283 system, NC-E-LT experiment, 2-ethyl-1-hexanol, ethyl benzoate, diethyl succinate and
284 phenol are again detected (Table 3). Ethoxy- and methoxy- substituted phenols together
285 with ethylcathecol are also identified. In the case of the water system, NC-W-LT
286 experiment, catechol, 2-ethyl-1-hexanol, phenol and ethyl catechol are the compounds
287 with the highest relative abundance. Alkylated and non-alkylated phenols, catechols and

guaiacols are also found in high concentrations (Table 3). Thus, the NC-E-LT oil contains a lower abundance of oxygenates, a lower abundance of dihydroxy-substituted phenols (i.e. sum of catechol, ethylcatechol and ethylcatechol).

**Table 3:** Semi-quantitative GC-MS analysis of the LT oils

| Compound | Experiment (Oil) | | | | | |
|---|---|---|---|---|---|---|
| | NC-E-LT | NC-W-LT | AC-E-LT | AC-W-LT | Ru-E-LT | Ru-W-LT |
| 2-ethyl-1-hexanol | 1.56 | 1.23 | 1.22 | 1.59 | 1.29 | 1.56 |
| Ethyl benzoate | 0.70 | –[a] | 0.57 | –[a] | 1.03 | –[a] |
| Diethyl succinate | 0.57 | –[a] | 0.57 | –[a] | 0.56 | –[a] |
| Phenol | 0.34 | 0.95 | 0.30 | 0.75 | 0.20 | 0.91 |
| o-Cresol | –[a] | 0.22 | –[a] | 0.21 | –[a] | 0.18 |
| p-Cresol | –[a] | 0.43 | –[a] | 0.41 | –[a] | 0.57 |
| p-Ethylphenol | –[a] | 0.71 | –[a] | 0.78 | –[a] | 0.95 |
| p-Propylphenol | –[a] | –[a] | –[a] | –[a] | –[a] | 0.46 |
| Catechol | –[a] | 1.51 | –[a] | 1.07 | –[a] | 0.87 |
| Methylcatechol | –[a] | 0.90 | –[a] | –[a] | –[a] | –[a] |
| Ethylcatechol | 1.28 | 0.93 | 0.94 | 0.52 | –[a] | 0.41 |
| Guaiacol | 0.56 | 0.71 | 0.58 | 0.70 | 0.31 | 0.56 |
| Ethylguaicol | 0.49 | 0.18 | 0.51 | 0.57 | 0.33 | 0.22 |
| Propylguaiacol | –[a] | –[a] | –[a] | –[a] | 0.26 | –[a] |
| Ethoxyphenol | 0.32 | –[a] | 0.28 | –[a] | 0.21 | –[a] |
| dMthdMtB[b] | 0.63 | –[a] | 0.70 | –[a] | –[a] | –[a] |
| 5-hydroxyindane | –[a] | 0.56 | –[a] | 0.37 | –[a] | 0.52 |
| EtProp[c] | –[a] | –[a] | –[a] | –[a] | –[a] | 0.47 |
| 2-Naphthalenol | –[a] | 0.40 | –[a] | 0.27 | –[a] | 0.25 |

[a]Low intensity peak or undetected compound [b]dMthdMtB: 1,4-Dimethoxy-2,3-dimethylbenzene [c]EtProp: 2′-Ethylpropiiophenone

For the AC experiments (Table 1, *entries 5-8*) the $M_w$ values of the oils produced for the ethanol system are again significantly higher than the ones produced for the water system (Figure 2, *above*). At HT the $M_w$ value of the AC-E-HT oil is of 340 Da, while only 225 Da for the AC-W-HT. At LT this difference is even higher, 483 Da for the ethanol system and 280 Da for the water system, respectively. No clear trend is

observed for the H/C and O/C ratio of the oils produced (Figure 2, *below*). At HT conditions, the ethanol system yields an oil with higher H/C ratio: 1.35 for the AC-E-HT and only 1.21 for the AC-W-HT. The O/C ratio is of 0.15 for both systems. At LT, on the other hand, the ethanol system yields oils with lower H/C and O/C ratios in comparison to the water system. As observed by GC-MS, there is no significant difference between the composition of the AC and NC oils (Table 2 and Table 3). At least among those compounds that could be identified. Only minor differences in the relative abundance of some of the components are detected, such as the larger amount of alkylated components (i.e. o-ethylphenol, p-ethylphenol, 2-ethyl-5-methylphenol and diethylphenol) found in the AC-E-HT experiment in comparison to the NC-E-HT experiment. The only remarkable compositional difference between the NC and AC oils is the absence of methylcatechol in the AC-W-LT oil.

For the experiments with the Ru/AC catalyst, higher $M_w$ values are again obtained for those oils produced in the presence of ethanol (Figure 2, *above*). At HT conditions, the $M_w$ values of the Ru-E-HT oil is of 415 Da while for the Ru-W-HT oil only 319 Da. At LT conditions, the Ru-E-LT and Ru-W-LT experiments yield oils with a $M_w$ of 498 Da and 360 Da, respectively. The O/C and H/C ratio of the Ru oil are comparable to the ones obtained for the AC oil. There are, however, considerable differences between the ethanol- and water-system oils. At HT, the ethanol system yields a more hydrodeoxygenated oil (Figure 2, *below*). The Ru-E-HT oil exhibits an H/C ratio of 1.33 and an O/C ratio of 0.14 while the Ru-W-HT oil exhibits an H/C and O/C ratio of 1.32 and 0.17, respectively. For the LT, the Ru-E-LT oil exhibits both a higher H/C and a higher O/C ratio than the Ru-W-LT oil (Figure 2, *below*).

The presence of the Ru/AC catalyst affects the final composition of the oils, as observed by GC-MS analysis. A higher abundance of alkyl-substituted compounds (i.e. higher

degree of alkylation) is detected in those oil produced in the presence of Ru/AC catalysts, especially in the case of the water system (Table 2 and Table 3). For the Ru-E-HT oil, more compounds are identified in comparison to its NC and AC counterparts. In addition to the compounds observed for the NC-E-HT and AC-E-HT oils, p-propylphenol, 1,4-dimethoxy-2,3-dimethylbenzene, propofol, 2-(1,1-dimethylethyl)-1,4-dimethoxybenzene and 1,2,4,5-tetraethylbenzene are detected (Table 2). In the case of the water system, Ru-W-HT additional compounds such as p-propylphenol, 1,2,3,5,6-pentamethylbenzene and 2′-ethylpropiophenone are also detected. Still, the main compositional differences between the ethanol and water system oils are maintained. At LT conditions, the compositional differences between the Ru and NC and AC oils are fewer (Table 3). The Ru-E-LT oil contains propylguaicol while no ethylcatechol or 2-(1,1-dimethylethyl)-1,4-dimethoxybenzene is detected. In the case of the water system, the Ru-W-LT oil also contains propylguaiacol and 2′-ethylpropiophenone while no methylcatechol is present as observed for the NC-W-LT and AC-W-LT.

340

341 *3.2.3 Effect of the type of solvent and the Ru/AC catalyst*

342 The LtL reaction sequential mechanism involves a series of successive reactions: (i)
343 aliphatic ether bond cleavage (i.e. lignin de-polymerization), (ii) stabilization of the
344 lignin fragments and/or (iii) lignin re-polymerization. In this mechanism formic acid
345 plays a double role, as already demonstrated in the literature (Oregui-Bengoechea et al.,
346 2017a): as catalyst for the de-polymerization of lignin and as hydrogen source for the
347 hydrodeoxygenation of lignin fragments. In the LtL reaction, the aliphatic ether bonds
348 of lignin are first cleaved through a formylation-deformylation-hydrogenolysis
349 mechanism leading to the depolymerization of the biopolymer into smaller lignin
350 fragments. Later, the produced lignin fragments either can re-polymerize into organic
351 solids (hydrochar) or can be stabilized through alkylation and hydrodeoxygenation
352 reactions. These stabilized lignin fragments have less tendency to re-polymerize,
353 leading to higher oil and lower solid yields (Forchheim et al., 2012; Gasson et al.,
354 2012). Hydrodeoxygenation of lignin fragments occurs due to the availability of
355 hydrogen resulting from the thermal decomposition of formic acid. Similar sequential
356 lignin conversion mechanisms have been reported in the literature (Gasson et al., 2012;
357 Huang et al., 2014; Kloekhorst and Heeres, 2015).

358 The results presented in *Section 3.2.1* and *Section 3.2.2* indicate that the type of solvent
359 (i.e. ethanol or water) and the presence of the Ru/AC catalyst have a significant effect
360 on the LtL reaction. The solvent effect on the oil and solid yield has already been
361 previously observed for the non-catalyzed LtL process (Løhre et al., 2016). The ethanol
362 system, in all cases, gives considerably higher oil yields than the water system. These
363 higher oil yields are generally accompanied by a reduction of the solid yield. This
364 positive effect induced by the ethanol solvent in the LtL-process could derive from

365 several causes: (i) the formation of ethanol-derived esters, (ii) ethyl-incorporation (C-
366 alkylation) and (iii) the stabilization of the de-polymerized lignin fragments. Besides, it
367 has to be taken into account that the oil yield in the water systems is slightly
368 underestimated. Some of the polar oil components found mostly in the water system
369 oils, catechols, are known to be soluble in water (Holmelid et al., 2017). During the
370 LtL-process work-up procedure the water phase, containing a fraction of those polar oil
371 components, is discharged.

372 As observed by GC-MS (Section 3.2.2), ethyl esters such as ethyl benzoate and diethyl
373 succinate are present only in those oils produced using ethanol as a solvent. Ethyl
374 benzoate is a product from the condensation of benzoic acid and ethanol. Diethyl
375 succinate, on the other hand, is formed from the esterification reaction between a
376 carboxylic acid (i.e. succinic acid) an ethanol. The GC-MS analysis also reveals that the
377 ethanol system oils have a higher abundance of ethyl-alkylated phenols. Ethanol can
378 also be incorporated in the produced lignin mono- and oligomer structures through C-
379 alkylation mechanisms (Holmelid et al., 2012; Løhre et al., 2016). These reactions will
380 contribute to an increase in the oil yield without any subsequent solid yield reduction.
381 This is the case of the Ru experiments at HT: the Ru-E-HT experiment give higher oil
382 yields than the Ru-W-HT experiment, but both yield comparable solid yields (Table 1).

383 However, the increase of the oil yield observed in the ethanol system is generally
384 accompanied by a reduction in the solid yield, especially in the LT experiments. As
385 already mentioned, hydrodeoxygenated and alkylated lignin mono- and oligomers tend
386 to have lesser tendency to re-polymerize. The GC-MS analysis shows that the
387 compounds found in the ethanol-system oils are more alkylated and
388 hydrodeoxygenated: they contain a larger amount of alkylated compounds and a smaller
389 amount of oxygenated compounds such as guaiacols and catechols. The analysis of the

390 $M_w$ values depicted in Figure 2 (*above*) also suggest that the ethanol system yields more
391 stable compounds. Higher $M_w$ oils are obtained when ethanol is used as a solvent, as
392 compared to the water system. This indicates that those high molecular weight
393 compounds found in the ethanol-system oils exhibit less tendency to re-polymerization,
394 and thus are more stable, than the ones produced in the presence of water. In water,
395 some of the large intermediates generated in the water system re-polymerize and end up
396 as part of the solid fraction. Thus, when using ethanol as a solvent, more stable (i.e.
397 hydroxygenated and alkylated) compounds are obtained, resulting in a higher oil and
398 lower solid yield.

399 As already mentioned, the presence of the Ru/AC catalyst, also significantly affects the
400 LtL process. The activity of the Ru/AC catalyst cannot be attributed to the AC support,
401 due to the similar oil and solid yields observed for the NC and AC experiments. The AC
402 bare support only exhibits a minor activity in the case of the ethanol system at HT
403 reaction conditions. This minor activity of the AC could be associated with its ability to
404 alkylate lignin fragments (Section 3.2.2). As mentioned above, lignin fragment (i.e.
405 monomer and/or oligomer) alkylation prevents their subsequent re-polymerization into
406 organic solids, resulting in a higher oil and a lower solid yield. This alkylation activity
407 could be a consequence of the general affinity of the ACs towards adsorption of liquid
408 and gas components from the LtL-reaction medium, and/or the activities of their
409 residual acid and basic surface functionalities, as discussed elsewhere (Oregui-
410 Bengoechea et al., 2017b).

411 In contrast, the presence of Ru considerably increases the oil and decreases the solid
412 yield in all cases (Figure 1). This considerable increase in lignin conversion is thought
413 to be a consequence of the hydrogenolysis, hydrodeoxgyenation and alkylation activity
414 of the $Ru^0$ active sites. The hydrogenolysis activity of Ru/AC catalyst has already been

reported in previous studies (Huang et al., 2018; Kloekhorst et al., 2015; M. Oregui Bengoechea et al., 2017). In addition, the results presented in Section 3.2.2 indicate that the Ru/AC catalyst exhibits considerable activity towards lignin fragment hydrodexoygenation and alkylation reactions (i.e. lignin fragment stabilization).

In a previous study, we measured the activity of a NiMo/AC and a NiMoFe/AC catalysts in the LtL process using ethanol as a solvent (Oregui-Bengoechea et al., 2017b). No experiments were performed in water given the significant deactivation that typical NiMo hydrotreating catalysts undergo under these reactions conditions (Laurent and Delmon, 1994; Etienne Laurent and Delmon, 1994). The Ru/AC catalyst is more active than the non-noble metal catalysts tested (i.e. NiMo/AC and NiMoFe/AC). At HT conditions, all the catalysts exhibit comparable activities, although the Ru/AC and NiMoFe/AC catalysts yield slightly larger amount of oil in comparison to the NiMo/AC. At LT conditions only the Ru/AC and the NiMoFe/AC catalyst exhibit activity. Still the best results are obtained for the Ru/AC catalyst with a slightly higher oil yield, 75.8 wt.%, and a slightly lower solid yield, 23.9 wt.%, in comparison to the NiMoFe/AC catalyst.

## 4. Conclusions

In comparison to the water system, the ethanol system yields a significantly larger amount of oil and, at 300 °C and 10 h, a smaller amount of solids due to the formation of ethanol-derived esters, C-alkylation of lignin fragments and the generation of more stable lignin derivatives. The activity of the $Ru^0$ active sites towards hydrogenolysis, hydrodeoxygenation and alkylation is the cause of the positive effect of the Ru/AC catalysts, inducing an oil yield increase and a solid yield decrease. Furthermore, $Ru^0$ has proven to be more active than Ni based catalysts, especially at low temperatures (i.e. 300 °C).

## Appendix A. Supplementary material

Supplementary material associated with this article can be found in the online version of the paper.


## Acknowledgements

This project was supported by the Lignoref project group (including The Research Council of Norway (grant no.190965/S60), Statoil ASA, Borregaard AS, Allskog BA, Cambi AS,Xynergo AS/Norske Skog, Hafslund ASA and Weyland AS) and by the Swedish Energy Agency and by VR and VINNOVA. The authors would also like to thank I. J. Fjellanger and Mali H. Rosnes for their assistance in the characterization of the oil and catalysts, and the Technical College of Bergen for supplying lignin. SGIker technical and human support (UPV/EHU, MINECO, GV/EJ, ERDF and ESF) is also gratefully acknowledged.


## Reference


1. Abioye, A.M., Ani, F.N., 2015. Recent development in the production of activated carbon electrodes from agricultural waste biomass for supercapacitors: A review. Renew. Sustain. Energy Rev. 52, 1282–1293. https://doi.org/http://dx.doi.org/10.1016/j.rser.2015.07.129
2. Azadfar, M., Gao, A.H., Chen, S., 2015. Structural characterization of lignin: A potential source of antioxidants guaiacol and 4-vinylguaiacol. Int. J. Biol. Macromol. 75, 58–66. https://doi.org/10.1016/j.ijbiomac.2014.12.049
3. Boorman, P.M., Kydd, R.A., Sorensen, T.S., Chong, K., Lewis, J.M., Bell, W.S., 1992. A comparison of alumina, carbon and carbon-covered alumina as supports for Ni□Mo□F additives: gas oil hydroprocessing studies. Fuel 71, 87–93. https://doi.org/http://dx.doi.org/10.1016/0016-2361(92)90197-V
4. Chandrakant, P., Bisaria, V.S., 1998. Simultaneous bioconversion of cellulose and hemicellulose to ethanol. Crit. Rev. Biotechnol. https://doi.org/10.1080/0738-

859891224185

5. Divakar, D., Manikandan, D., Rupa, V., Preethi, E.L., Chandrasekar, R., Sivakumar, T., 2007. Palladium-nanoparticle intercalated vermiculite for selective hydrogenation of α,β-unsaturated aldehydes. J. Chem. Technol. Biotechnol. 82, 253–258. https://doi.org/10.1002/jctb.1661
6. Forchheim, D., Gasson, J.R., Hornung, U., Kruse, A., Barth, T., 2012. Modeling the Lignin Degradation Kinetics in a Ethanol/Formic Acid Solvolysis Approach. Part 2. Validation and Transfer to Variable Conditions. Ind. Eng. Chem. Res. 51, 15053–15063. https://doi.org/10.1021/ie3026407
7. Gasson, J.R., Forchheim, D., Sutter, T., Hornung, U., Kruse, A., Barth, T., 2012. Modeling the Lignin Degradation Kinetics in an Ethanol/Formic Acid Solvolysis Approach. Part 1. Kinetic Model Development. Ind. Eng. Chem. Res. 51, 10595–10606. https://doi.org/10.1021/ie301487v
8. Hao, W., Björnerbäck, F., Trushkina, Y., Bengoechea, M.O., Salazar-Alvarez, G., Barth, T., Hedin, N., 2017. High-performance Magnetic Activated Carbon from Solid Waste from Lignin Conversion Processes. Part I: Their Use as Adsorbents for CO2, in: Energy Procedia. https://doi.org/10.1016/j.egypro.2017.08.033
9. Hao, W., Keshavarzi, N., Branger, A., Bergström, L., Hedin, N., 2014. Strong discs of activated carbons from hydrothermally carbonized beer waste. Carbon N. Y. 78, 521–531. https://doi.org/http://dx.doi.org/10.1016/j.carbon.2014.07.036
10. Hayes, D.J., Fitzpatrick, S., Hayes, M.H.B., Ross, J.R.H., 2008. The Biofine Process - Production of Levulinic Acid, Furfural, and Formic Acid from Lignocellulosic Feedstocks, in: Biorefineries-Industrial Processes and Products: Status Quo and Future Directions. pp. 139–164. https://doi.org/10.1002/9783527619849.ch7
11. Holmelid, B., Barth, T., Brusletto, R., Kleinert, M., 2017. Production of monomeric phenols by formic acid assisted hydrous liquefaction of lignin. Biomass and Bioenergy 105, 298–309. https://doi.org/10.1016/j.biombioe.2017.07.017
12. Holmelid, B., Kleinert, M., Barth, T., 2012. Reactivity and reaction pathways in

493 thermochemical treatment of selected lignin-like model compounds under hydrogen rich
494 conditions. J. Anal. Appl. Pyrolysis 98, 37–44.
495 https://doi.org/http://dx.doi.org/10.1016/j.jaap.2012.03.007
496 13. Huang, X., Korányi, T.I., Boot, M.D., Hensen, E.J.M., 2014. Catalytic Depolymerization of
497 Lignin in Supercritical Ethanol. ChemSusChem 7, 2276–2288.
498 https://doi.org/10.1002/cssc.201402094
499 14. Huang, Y., Duan, Y., Qiu, S., Wang, M., Ju, C., Cao, H., Fang, Y., Tan, T., 2018. Lignin-
500 first biorefinery: a reusable catalyst for lignin depolymerization and application of lignin oil
501 to jet fuel aromatics and polyurethane feedstock. Sustain. Energy Fuels.
502 https://doi.org/10.1039/C7SE00535K
503 15. IEA, 2012. World Energy Outlook 2012, International Energy Agency.
504 https://doi.org/10.1787/20725302
505 16. J??nsson, L.J., Alriksson, B., Nilvebrant, N.O., 2013. Bioconversion of lignocellulose:
506 Inhibitors and detoxification. Biotechnol. Biofuels. https://doi.org/10.1186/1754-6834-6-16
507 17. Kleinert, M., Barth, T., 2008. Phenols from lignin. Chem. Eng. Technol. 31, 736–745.
508 https://doi.org/10.1002/ceat.200800073
509 18. Kleinert, M., Gasson, J.R., Barth, T., 2009. Optimizing solvolysis conditions for integrated
510 depolymerisation and hydrodeoxygenation of lignin to produce liquid biofuel. J. Anal.
511 Appl. Pyrolysis 85, 108–117. https://doi.org/http://dx.doi.org/10.1016/j.jaap.2008.09.019
512 19. Kloekhorst, A., Heeres, H.J., 2015. Catalytic Hydrotreatment of Alcell Lignin Using
513 Supported Ru, Pd, and Cu Catalysts. ACS Sustain. Chem. Eng. 3, 1905–1914.
514 https://doi.org/10.1021/acssuschemeng.5b00041
515 20. Kloekhorst, A., Shen, Y., Yie, Y., Fang, M., Heeres, H.J., 2015. Catalytic
516 hydrodeoxygenation and hydrocracking of Alcell® lignin in alcohol/formic acid mixtures
517 using a Ru/C catalyst. Biomass and Bioenergy 80, 147–161.
518 https://doi.org/http://dx.doi.org/10.1016/j.biombioe.2015.04.039
519 21. Kowalczyk, Z., Stołecki, K., Raróg-Pilecka, W., Miśkiewicz, E., Wilczkowska, E.,
520 Karpiński, Z., 2008. Supported ruthenium catalysts for selective methanation of carbon

521 oxides at very low COx/H2ratios. Appl. Catal. A Gen. 342, 35–39.
522 https://doi.org/10.1016/j.apcata.2007.12.040
523 22. Lange, H., Decina, S., Crestini, C., 2013. Oxidative upgrade of lignin - Recent routes
524 reviewed, in: European Polymer Journal. pp. 1151–1173.
525 https://doi.org/10.1016/j.eurpolymj.2013.03.002
526 23. Laurent, E., Delmon, B., 1994. Deactivation of a Sulfided NiMo/??-Al2O3 during the
527 Hydrodeoxygenation of Bio-Oils: Influence of a High Water Pressure. Stud. Surf. Sci.
528 Catal. 88, 459–466. https://doi.org/10.1016/S0167-2991(08)62773-1
529 24. Laurent, E., Delmon, B., 1994. Influence of water in the deactivation of a sulfided NiMo γ-
530 Al2O3 catalyst during hydrodeoxygenation. J. Catal. 146. https://doi.org/10.1016/0021-
531 9517(94)90032-9
532 25. Li, C., Zhao, X., Wang, A., Huber, G.W., Zhang, T., 2015. Catalytic Transformation of
533 Lignin for the Production of Chemicals and Fuels. Chem. Rev. 115, 11559–11624.
534 https://doi.org/10.1021/acs.chemrev.5b00155
535 26. Liguori, L., Barth, T., 2011. Palladium-Nafion SAC-13 catalysed depolymerisation of lignin
536 to phenols in formic acid and water. J. Anal. Appl. Pyrolysis 92, 477–484.
537 https://doi.org/http://dx.doi.org/10.1016/j.jaap.2011.09.004
538 27. Liu, W.-J., Zhang, X.-S., Qv, Y.-C., Jiang, H., Yu, H.-Q., 2012. Bio-oil upgrading at
539 ambient pressure and temperature using zero valent metals. Green Chem. 14, 2226.
540 https://doi.org/10.1039/c2gc35426h
541 28. Løhre, C., Barth, T., Kleinert, M., 2016. The effect of solvent and input material
542 pretreatment on product yield and composition of bio-oils from lignin solvolysis. J. Anal.
543 Appl. Pyrolysis 119, 208–216. https://doi.org/http://dx.doi.org/10.1016/j.jaap.2016.03.003
544 29. Nie, L., de Souza, P.M., Noronha, F.B., An, W., Sooknoi, T., Resasco, D.E., 2014. Selective
545 conversion of m-cresol to toluene over bimetallic Ni–Fe catalysts. J. Mol. Catal. A Chem.
546 388–389, 47–55. https://doi.org/http://dx.doi.org/10.1016/j.molcata.2013.09.029
547 30. Oregui-Bengoechea, M., Gandarias, I., Arias, P.L., Barth, T., 2017a. Unraveling the Role of
548 Formic Acid and the Type of Solvent in the Catalytic Conversion of Lignin: A Holistic

549 Approach. ChemSusChem n/a-n/a. https://doi.org/10.1002/cssc.201601410
550 31. Oregui-Bengoechea, M., Gandarias, I., Miletić, N., Simonsen, S.F., Kronstad, A., Arias,
551 P.L., Barth, T., 2017. Thermocatalytic conversion of lignin in an ethanol/formic acid
552 medium with NiMo catalysts: Role of the metal and acid sites. Appl. Catal. B Environ. 217.
553 https://doi.org/10.1016/j.apcatb.2017.06.004
554 32. Oregui-Bengoechea, M., Miletić, N., Hao, W., Björnerbäck, F., Rosnes, M.H.,
555 Garitaonandia, J.S., Hedin, N., Arias, P.L., Barth, T., 2017b. High-Performance Magnetic
556 Activated Carbon from Solid Waste from Lignin Conversion Processes. 2. Their Use as
557 NiMo Catalyst Supports for Lignin Conversion. ACS Sustain. Chem. Eng. 5, 11226–11237.
558 33. Oregui Bengoechea, M., Hertzberg, A., Miletić, N., Arias, P.L., Barth, T., 2015.
559 Simultaneous catalytic de-polymerization and hydrodeoxygenation of lignin in water/formic
560 acid media with Rh/Al<inf>2</inf>O<inf>3</inf>,
561 Ru/Al<inf>2</inf>O<inf>3</inf> and
562 Pd/Al<inf>2</inf>O< J. Anal. Appl. Pyrolysis 113.
563 https://doi.org/10.1016/j.jaap.2015.04.020
564 34. Oregui Bengoechea, M., Miletï¿½c, N., Vogt, M.H., Arias, P.L., Barth, T., 2017. Analysis
565 of the effect of temperature and reaction time on yields, compositions and oil quality in
566 catalytic and non-catalytic lignin solvolysis in a formic acid/water media using
567 experimental design. Bioresour. Technol. https://doi.org/10.1016/j.biortech.2017.02.129
568 35. Oregui Bengoechea, M., Miletíc, N., Vogt, M.H., Arias, P.L., Barth, T., 2017. Analysis of
569 the effect of temperature and reaction time on yields, compositions and oil quality in
570 catalytic and non-catalytic lignin solvolysis in a formic acid/water media using
571 experimental design. Bioresour. Technol. 234.
572 https://doi.org/10.1016/j.biortech.2017.02.129
573 36. Pepper, J.M., Lee, Y.W., 1969. Lignin and related compounds. I. A comparative study of
574 catalysts for lignin hydrogenolysis. Can. J. Chem. 47, 723–727. https://doi.org/10.1139/v69-
575 118
576 37. Popa, V.I., 2018. 1 – Biomass for Fuels and Biomaterials, in: Biomass as Renewable Raw

577 Material to Obtain Bioproducts of High-Tech Value. pp. 1–37.
578 https://doi.org/10.1016/B978-0-444-63774-1.00001-6
579 38. Rossetti, I., Pernicone, N., Forni, L., 2003. Characterisation of Ru/C catalysts for ammonia
580 synthesis by oxygen chemisorption. Appl. Catal. A Gen. 248, 97–103.
581 https://doi.org/10.1016/S0926-860X(03)00151-0
582 39. Suhas, Carrott, P.J.M., Ribeiro Carrott, M.M.L., 2007. Lignin – from natural adsorbent to
583 activated carbon: A review. Bioresour. Technol. 98, 2301–2312.
584 https://doi.org/http://dx.doi.org/10.1016/j.biortech.2006.08.008
585 40. Vissers, J.P.R., Scheffer, B., de Beer, V.H.J., Moulijn, J.A., Prins, R., 1987. Effect of the
586 support on the structure of Mo-based hydrodesulfurization catalysts: Activated carbon
587 versus alumina. J. Catal. 105, 277–284. https://doi.org/http://dx.doi.org/10.1016/0021-
588 9517(87)90058-3
589 41. Wang, W., Yang, Y., Luo, H., Peng, H., He, B., Liu, W., 2011. Preparation of Ni(Co)-W-B
590 amorphous catalysts for cyclopentanone hydrodeoxygenation. Catal. Commun. 12, 1275–
591 1279. https://doi.org/10.1016/j.catcom.2011.04.027
592 42. Xu, W., Miller, S.J., Agrawal, P.K., Jones, C.W., 2012. Depolymerization and
593 Hydrodeoxygenation of Switchgrass Lignin with Formic Acid. ChemSusChem 5, 667–675.
594 https://doi.org/10.1002/cssc.201100695
595 43. Zakzeski, J., Bruijnincx, P.C.A., Jongerius, A.L., Weckhuysen, B.M., 2010. The Catalytic
596 Valorization of Lignin for the Production of Renewable Chemicals. Chem. Rev. 110, 3552–
597 3599. https://doi.org/10.1021/cr900354u

598

**Appendix A. Supplementary material:**

# Solvent and catalyst effect in the formic acid aided Lignin-to-liquids

Mikel Oregui-Bengoechea*[a,b], Inaki Gandarias[b], Pedro L. Arias[b] and Tanja Barth[a]

[a] *Department of Chemistry, University of Bergen, Allégaten 41, 5007 Bergen, Norway*

[b] *Department of Chemical and Environmental Engineering, School of Engineering, University of the Basque Country (EHU/UPV), C/Alameda Urquijo s/n,48013 Bilbao, Spain*

**INDEX**

## LIGNIN ASH CONTENT

Three crucibles were calcined at 575 °C and weighed to the nearest 0.1 mg until constant weight (less than ±0.3 mg after one 1 h of heating at 575 °C). Once the weight of each crucible is recorded, between 0.5 and 2.0 g of lignin was weighed into each tared crucible. The lignin was calcined using the following temperature program: hold the temperature at 105 °C for 12 min, increase the temperature until 250 °C at 10 °C/min, hold the temperature at 250 °C for 30 min, increase the temperature until 575 °C at 20 °C/min, and hold it at that temperature for 180 min. After cooling, the samples were weighed to the nearest of 0.1 mg weighted until constant weight. The final ash content is calculated as the mean of the three crucibles.

## CATALYST CHARACTERIZATION

*$N_2$-adsorption:* $N_2$-adsorption measurements were carried out on a BELSORP-max instrument equipped with a low pressure transducer and a turbomolecular pump, allowing measurements with high precision from very low pressures ($p/p_0 = 10^{-8}$ mbar). The nitrogen adsorption isotherms were recorded at 77 K. The samples were degassed under conditions of dynamic vacuum at a temperature of 150 ºC overnight, before conducting the adsorption experiments.

Specific surface areas ($S_{BET}$) were calculated in the Brunauer–Emmet–Teller (BET) model, using the uptake of $N_2$ at relative pressures of $p/p_0 = 0.06 - 0.29$. Care was taken to assure positive and not unphysically large c-values.

*X-ray diffraction (XRD):* XRD patterns were collected by using a PHILIPS X'PERT PRO automatic diffractometer operating at 40 kV and 40 mA, in theta–theta configuration, a secondary monochromator with Cu-Kα radiation (λ = 1.5418 Å) and a PIXcel solid state detector (active length in $2\theta = 3.347$ °). Data were collected from 10 to 80° $2\theta$ (step size = 0.02606 and time per step = 600 s) at RT. Fixed divergence and anti-scattering slits giving a constant volume of sample illumination were used.

*Temperature-program reduction (TPR):* TPR was carried out in a chemisorption analyzer AutoChem II (Micromeritics, USA) equipped with a thermal conductivity detector. The non-activated Ru/AC catalyst (100 mg) was previously outgassed at 450 °C for 30 min. Later, the sample was exposed to a constant flow of 5% $H_2$ in argon, while being heated from room temperature to 450 °C with heating rate of 10 °C/min.

*CO-Chemisorption:* CO-chemisorption was carried out in an AutoChem (Micromeritics) device equipped with a calibrated TCD detector. The catalyst sample (55,7 mg) was placed in a U shaped quartz cell. Prior to measurements, the sample was reduced in a $H_2$/Ar ((5/95 vol/vol) flow (40 mL/min) at 300 ˚C for 1 h. Later, the sample was flushed with He and cooled down to 35 °C. At this temperature, CO pulses were injected to the sample until saturation was observed.

*Inductively coupled plasma atomic emission spectroscopy (ICP-AES):* ICP-AES was carried out using an Optima 2000-DV, Perkin Elmer, USA. Prior to measurements, the samples were dissolved in an HCl / $HNO_3$ acid mixture (volume ratio 3:1), digested in a microwave oven for 2 h and diluted with deionized water to concentrations within the detection range of the instrument.

## CHARACTERIZATION OF THE OIL

*Elemental Analysis:* The elemental composition of the samples were determined in the CHNS mode with a Vario EL III instrument using helium as carrier gas. The amount of oxygen was calculated by difference. The H/C and O/C are given in molar ratios.

*GPC-SEC:* The sample (1 mg) was dissolved in 1 mL of THF. The solution (20 μL) was injected into a GPC-SEC system equipped with a PLgel 3μm Mini MIX-E column, and analyzed at a flow rate of 0.5 mL/min of THF at 21.1 °C. The detection was performed with UV detector at 254 and 280 nm, as well as with a RI detector. The set of columns was calibrated with a series of polystyrene standards covering a molecular-mass range of 162–2360 Da. The average molecular weight of the oils ($M_w$) was calculated based on their retention times (min), time of the maximum of the eluted peak, with the aid of a series of polystyrene standards covering a molecular-mass range of 162–2360 Da. Due to very similar peak shapes, the polydispersity and molecular weight distribution of the oils was not considered.

*GC-MS:* The LtL-oil was analyzed on a 5977A Series GC/MSD system from Agilent Technologies. A EtAc:THF (90:10) mixture containing hexadecane as internal standard (2 μL/L) was used as solvent and the samples (1 mg of oil/1mL of solvent) were analyzed using splitless injection at 280 °C (injector temperature) on a 30 m HP-5MS capillary column ((5% phenyl)-methylpolysiloxane), 0.250 mm ID from Agilent Technologies. A constant gas flow rate of 1 mL/min and the following GC oven temperature program were applied: 40 °C for 5 min, followed by a heating ramp of 6 °C/min from 40 °C to 280 °C and a heating ramp of 40 °C/min from 280 °C to 300 °C. The GC–MS interphase valve delay was set to 5 min and the MS detector operated in positive mode at 70 eV with an ion-source temperature of 250 °C. Compounds were identified using the ChemStation software and the NIST 2.0 library.

The semi-quantitative GC-MS analysis was performed by integrating the peak for each compound and comparing this value with the internal standard peak area. Thus, the relative abundance of a compound ($A_i/A_s$) is defined as the ratio between the areas of the peak for a certain compound ($A_i$) and the area of the internal standard peak ($A_s$).

**Table S1:** Amount of reactants for the LtL experiments

| Experiment A[a]-B[b]-X[c] | Temperature (°C) | Reaction time (h) | Lignin (g.) | Lignin[d] (wt.%) | Solvent[d] (wt.%) | FA[d] (wt.%) | Catalyst[d] (wt.%) |
|---|---|---|---|---|---|---|---|
| NC-E-HT | 340 | 6 | 2.0 | 33.3 | 41.9 | 24.8 | 0.0 |
| NC-W-HT | 340 | 6 | 2.0 | 33.0 | 41.7 | 25.3 | 0.0 |
| NC-E-LT | 300 | 10 | 2.0 | 33.2 | 41.7 | 25.1 | 0.0 |
| NC-W-LT | 300 | 10 | 2.0 | 32.9 | 41.7 | 25.4 | 0.0 |
| AC-E-HT | 340 | 6 | 2.0 | 32.4 | 40.5 | 23.9 | 3.2 |
| AC-W-HT | 340 | 6 | 2.0 | 31.8 | 40.4 | 24.6 | 3.2 |
| AC-E-LT | 300 | 10 | 2.0 | 32.1 | 40.5 | 24.2 | 3.2 |
| AC-W-LT | 300 | 10 | 2.0 | 31.9 | 40.8 | 24.1 | 3.2 |
| Ru-E-HT | 340 | 6 | 2.0 | 32.1 | 40.2 | 24.5 | 3.2 |
| Ru-W-HT | 340 | 6 | 2.0 | 31.9 | 40.5 | 24.4 | 3.2 |
| Ru-E-LT | 300 | 10 | 2.0 | 32.0 | 40.3 | 24.5 | 3.2 |
| Ru-W-LT | 300 | 10 | 2.0 | 31.9 | 40.6 | 24.3 | 3.2 |

[a] Type of catalyst: non-catalyzed (NC), bare activated carbon (AC) and activated Ru/AC catalyst (Ru) [b] Type of solvent: ethanol (E) or water (W) [c] Reaction conditions: 340 °C and 6 h (HT) and 300 °C and 10 h (LT) [d] Average value of the replicates

**Table S2:** surface area ($S_{BET}$), Ru loading (ICP-AES) and number of Ru active sites of the AC and Ru/AC catalysts

| Catalyst[a] | $S_{BET}$ ($m^2/g$) | Ru loading (wt.%) | Number of $Ru^0$ active sites (μmol/g cat) |
|---|---|---|---|
| AC | 1415[b] | – | – |
| Ru/AC | 1185 | 3.7 | 7.3 |

[a] Catalyst: activated carbon bare support (AC) and $H_2$-activated Ru/AC catalyst (Ru/AC) [b] These values have already been reported in a previous study (Mikel Oregui-Bengoechea et al., 2017b)

**Table S3:** Oil and solid yields for the NiMo/C, NiMoFe/C and Ru/AC catalysts

| Entry | Experiment A[a]-B[b] | Oil Yield (wt.%)[d,e] | Solid Yield (wt.%)[d,e] |
|---|---|---|---|
| 1 | NC-HT | 36.0 | 43.6 |
| 2 | NiMo/AC-HT | 67.6 | 20.1 |
| 3 | NiMoFe/AC-HT | 72.1 | 21.1 |
| 4 | Ru/AC-HT | 72.0 | 22.9 |
| 5 | NC-LT | 49.3 | 28.3 |
| 6 | NiMo/AC-LT | 49.2 | 26.2 |
| 7 | NiMoFe/AC-LT | 72.0 | 27.7 |
| 8 | Ru/AC-LT | 75.8 | 23.9 |

[a] Type of catalyst: non-catalyzed experiment (NC), NiMo/AC catalyzed experiment (NiMo/AC), NiMoFe catalyzed experiment (NiMoFe/AC) and Ru/AC catalyzed experiment (Ru/AC) [b] Reaction conditions: 340 °C and 6 h (HT) and 300 °C and 10 h (LT) [d] Relative to lignin input [e] Average value of the replicates

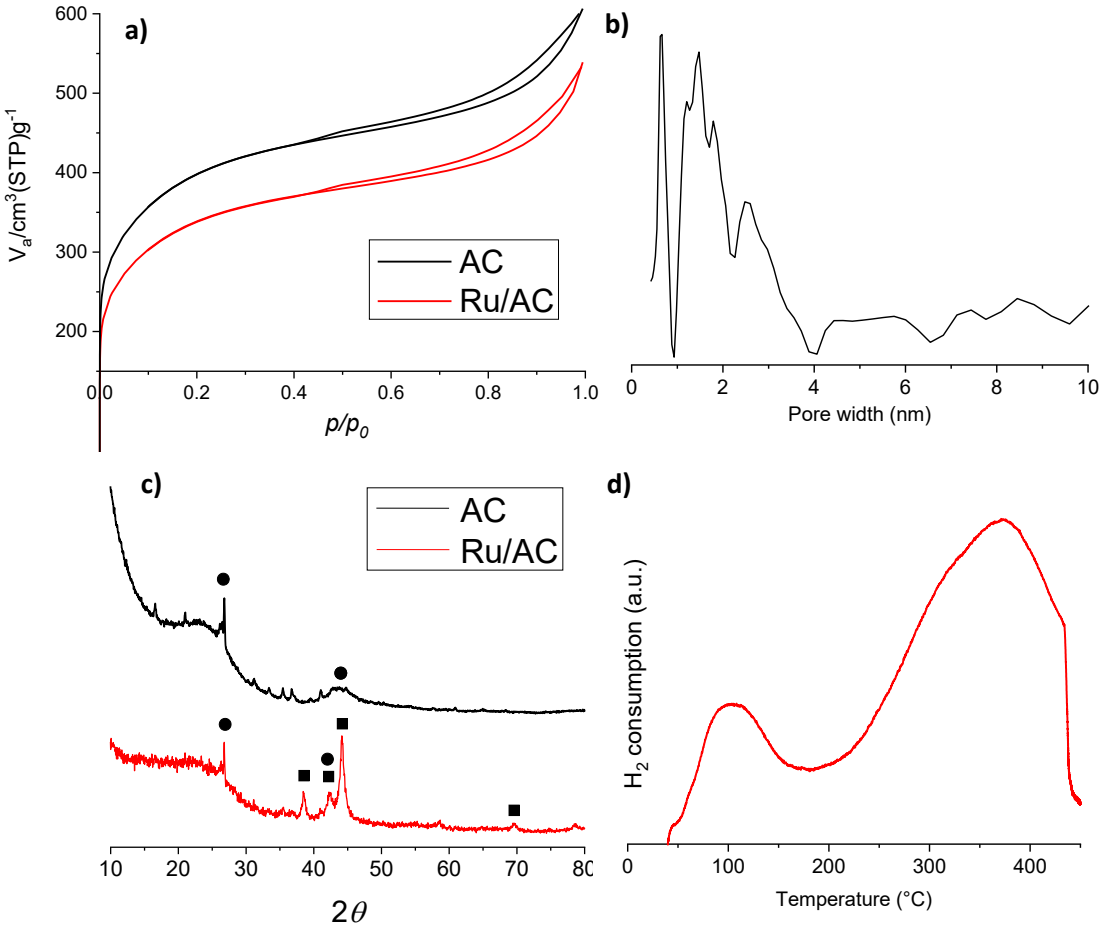


Figure S1. (a) $N_2$-adsorption-desorption isotherms for AC bare support (black) and Ru/AC (red) catalyst. (b) Pore size distribution for the AC bare support using DFT model. (c) X-ray diffraction patterns for AC bare support (black) and Ru/AC catalysts (red). Hexagonal $Ru^0$ structure (■) and AC related signals (●). (d) TPR profile for the non-activated Ru/AC catalyst. $N_2$-adsorption results and pore size distribution for the AC bare support have already been reported in a previous study (Mikel Oregui-Bengoechea et al., 2017b)

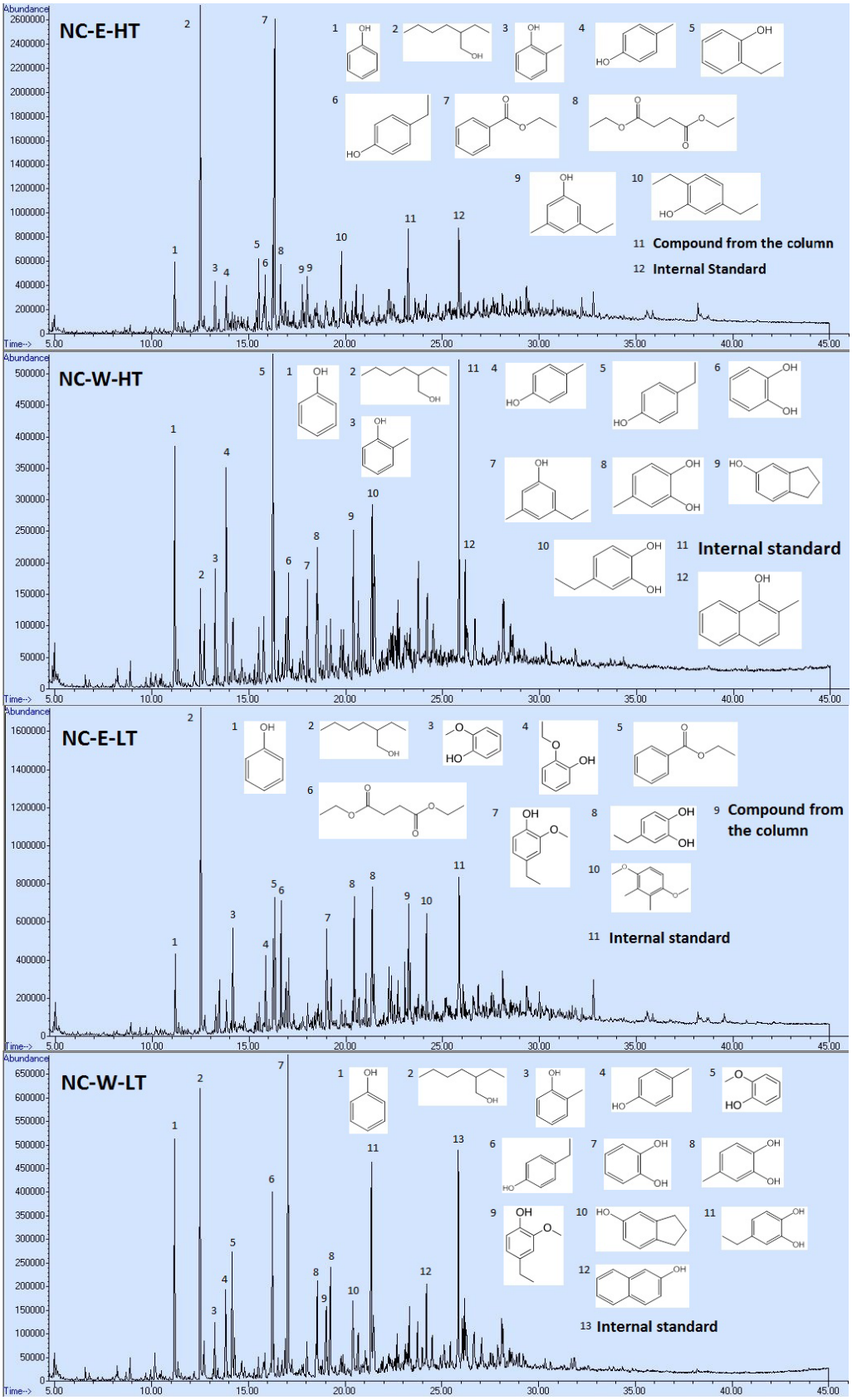
NC-E-HT
11 Compound from the column
12 Internal Standard
NC-W-HT
11 Internal standard
NC-E-LT
9 Compound from the column
11 Internal standard
NC-W-LT
13 Internal standard
Abundance
Time-->

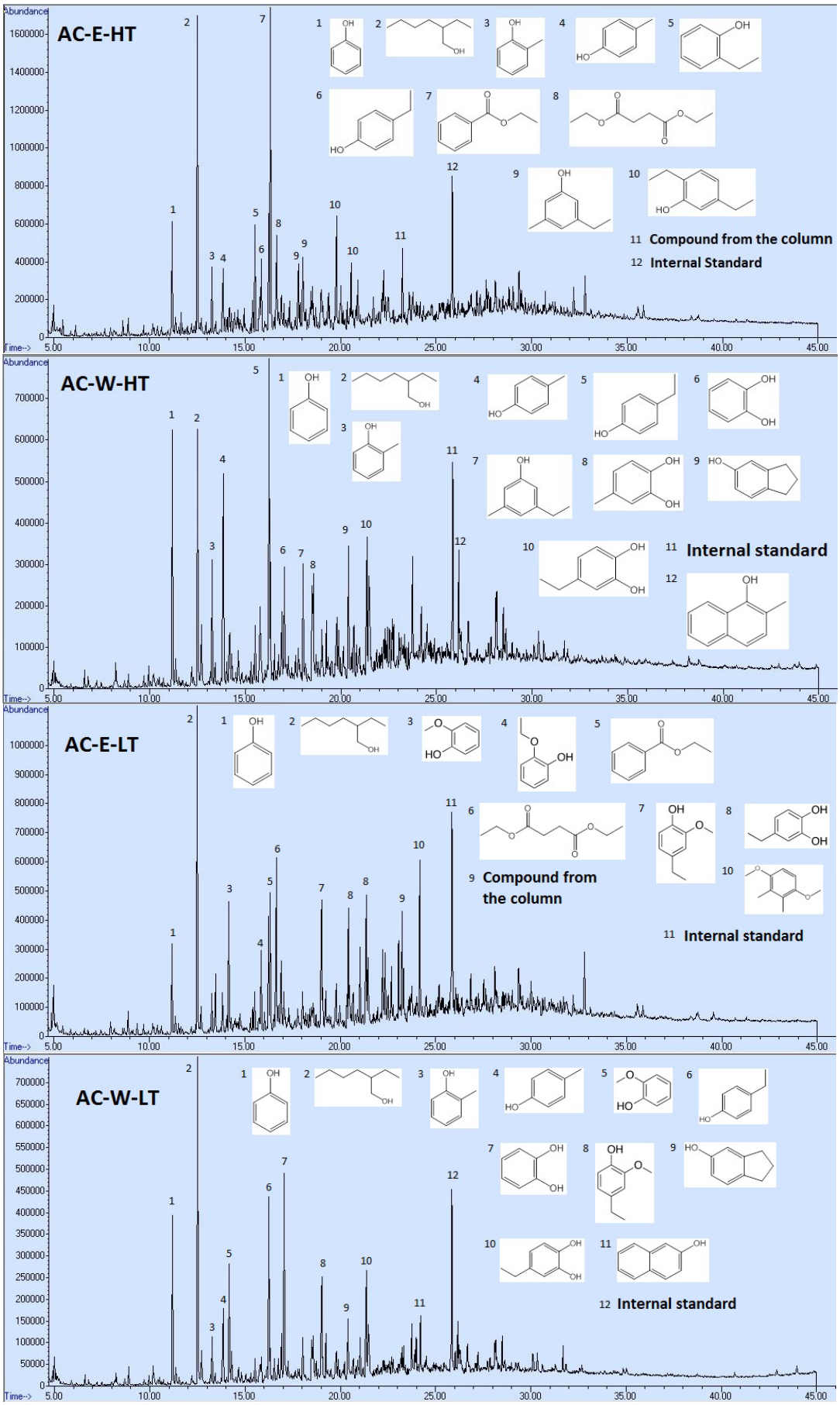
AC-E-HT
11 Compound from the column
12 Internal Standard
AC-W-HT
11 Internal standard
AC-E-LT
9 Compound from the column
11 Internal standard
AC-W-LT
12 Internal standard
Abundance
Time-->

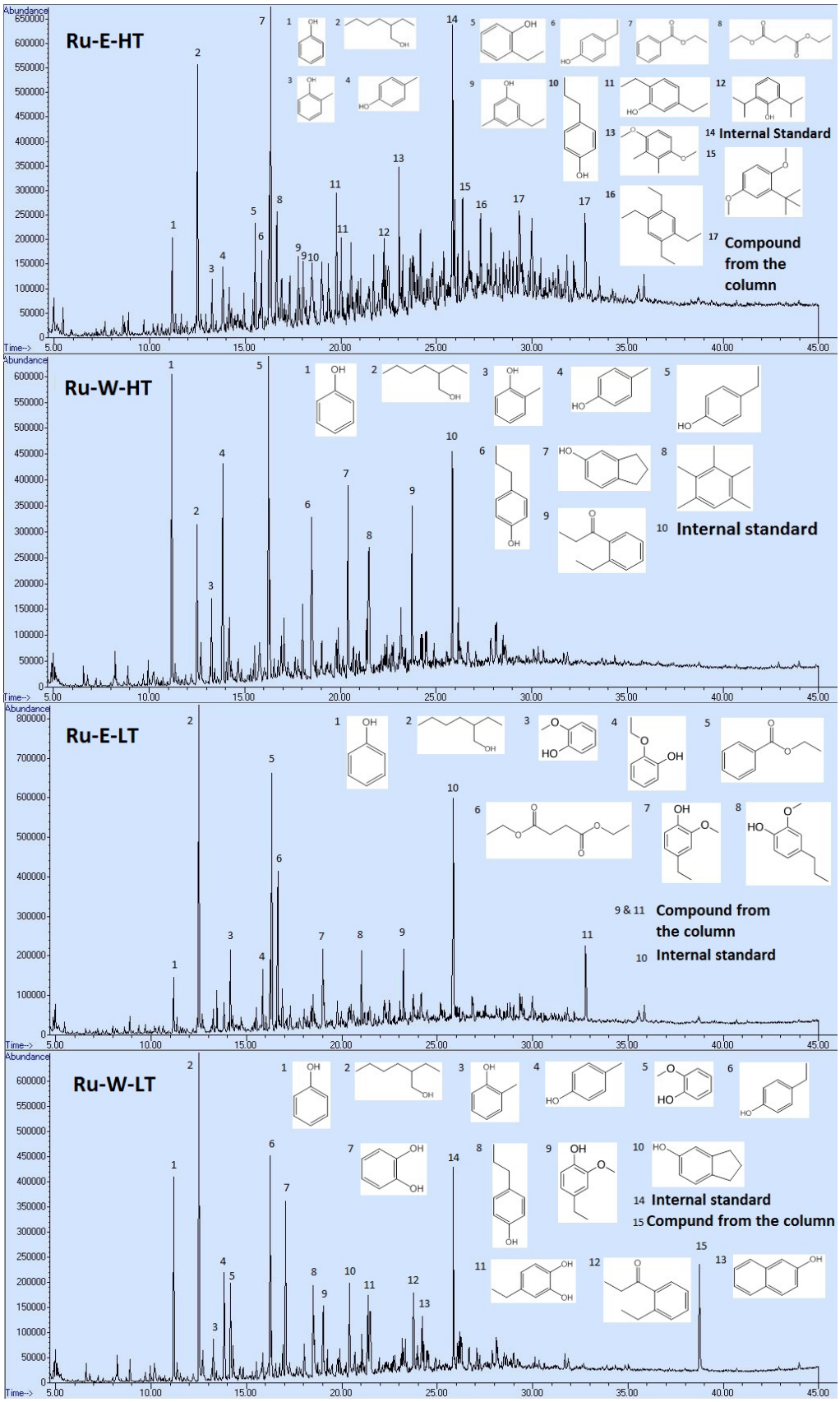


**Figure S2.** GC-MS chromatograms of the NC-E-HT, NC-W-HT, NC-E-LT, NC-W-LT, AC-E-HT, AC-W-HT, AC-E-LT, AC-W-LT, Ru-E-HT, Ru-W-HT, Ru-E-LT, Ru-W-LT

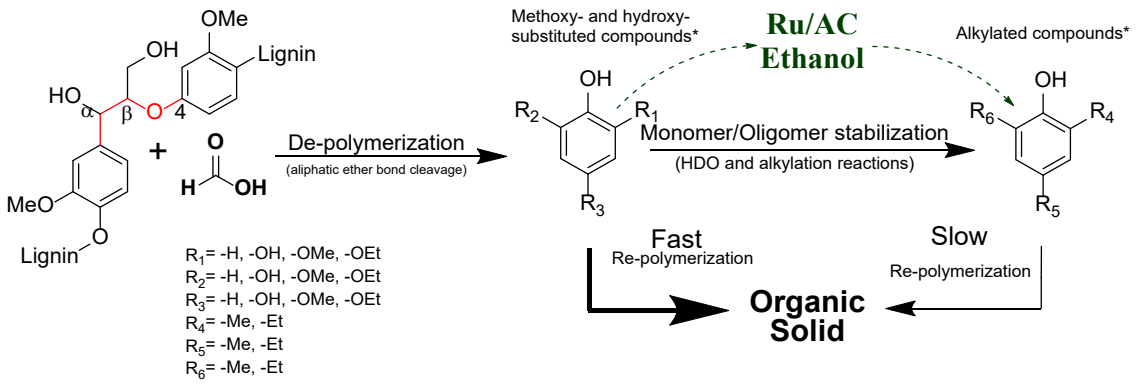


Scheme 1. Sequential reaction scheme for the conversion of lignin into bio-oil. The dashed lines represent reactions that are more favored in in the presence of a Ru/AC catalyst and/or using ethanol as solvent than in the absence of catalysts and/or using water as solvent.